JOURNAL OF AGRICULTURAL AND FOOD CHEMISTRY

Molecular Structure of Selected Tuber and Root Starches and Effect of Amylopectin Structure on Their Physical Properties

SANG-HO YOO,[†] CHANDANI PERERA,[‡] JIANFU SHEN,[§] LIYANG YE,[§] DONG-SOON SUH,[‡] AND JAY-LIN JANE*,[‡]

Department of Food Science and Technology, Sejong University, 98 Gunja-Dong, Gwangjin-Gu, Seoul 143-747, Korea; Department of Food Science and Human Nutrition and Center for Crops Utilization and Research, Iowa State University, Ames, Iowa 50010; and Department of Food Science and Technology, Zhejiang University, Hangzhou, China

The objectives of this study were to characterize starches isolated from potato, canna, fern, and kudzu, grown in Hangzhou, China, for potential food and nonfood applications and to gain understandings of the structures and properties of tuber and root starches. Potato and canna starches with B-type X-ray patterns had larger proportions of amylopectin (AP) long branch chains (DP ≥37) than did fern (C-type) and kudzu (C_A-type) starches. The analysis of Naegeli dextrins suggested that fern and kudzu starches had more branch points, α-(1,6)-D-glycosidic linkages, located within the double-helical crystalline lamella than did the B-type starches. Dispersed molecular densities of the C- and C_A-type APs (11.6−13.5 g/mol/nm^3) were significantly larger than those of the B-type APs (1.4−6.1 g/mol/nm^3) in dilute solutions. The larger proportion of the long AP branch chains in the B-type starch granules resulted in greater gelatinization enthalpy changes (ΔH). Retrograded kudzu starch, which had the shortest average chain length (DP 25.1), melted at a lower temperature (37.9 °C) than the others. Higher peak viscosities (550−749 RVU at 8%, dsb) of potato starches were attributed to the greater concentrations of phosphate monoesters, longer branch chains, and larger granule sizes compared with other tuber and root starches.

KEYWORDS: Amylose; amylopectin; molecular weight; dispersed molecular density; gelatinization; retrogradation; pasting

INTRODUCTION

Starch consists of two polysaccharides, primarily linear amylose (AM) and branched amylopectin (AP). AMs are relatively small molecules with a few branches, whereas APs are highly branched large molecules with molecular weights of 10^7-10^9 g/mol (*1*). APs consist of linear chains of α-(1,4)-D-glucose units branched by α-(1,6)-D-glycosidic linkages (*2*). Depending on the botanical source, the AM/AP ratio varies, and this affects the starch properties (*3*). Branch chain lengths of AP and molecular sizes of AM control the viscosity of starch paste (*4*). Ong and Blanshard (*5*) reported that AP structure and AM content affected the texture of cooked rice. Takeda et al. (*6*) showed that the long AP chains, mimicking AM, were responsible for the texture of *indica* rice.

Normal starches have been reported to contain 20−36% of AM (*7*). The values of AM content reported in the literature are mostly apparent AM contents, which were determined using iodine affinity (IA). Because long branch chains of AP can also form helical complexes with iodine, Kasemsuwan et al. (*8*) and Jane et al. (*3*) reported that the long chains of AP in the starch resulted in a greater iodine affinity and thus a higher apparent amylose content of starch. AP is the major component of normal starches, and the branch chain length distribution of AP is a characteristic of its botanical source. Hizukuri et al. (*9*) related the AP chain length to the polymorph of starch. It has also been shown that the growth conditions of the plant and lipid contents affect the polymorphism (*9, 10*). Different unit cells of packing AP double-helical branch chains give distinct A- and B-type X-ray diffraction patterns (*11*). The C-type is a mixture of the A- and B-type patterns (*12*). The APs of the A-type polymorphic starch have shorter average chain lengths and larger proportions of short chains (DP 6−12); those of the B-type polymorphic starch have longer average chain lengths and smaller proportions of short chains. APs of the C-type starch have intermediate average branch chain lengths and larger proportions of both short (DP 6−12) and long (DP ≥37) chains (*3, 9, 13, 14*). Starches with smaller proportions of long branch chains display lower gelatinization temperatures, less enthalpy changes (*3, 4, 15, 16*),

* Author to whom correspondence should be addressed [telephone (515) 294-9892; fax (515) 294-8181; e-mail jjane@iastate.edu].
[†] Sejong University.
[‡] Iowa State University.
[§] Zhejiang University.

10.1021/jf802960f CCC: $40.75
Published on Web 01/30/2009

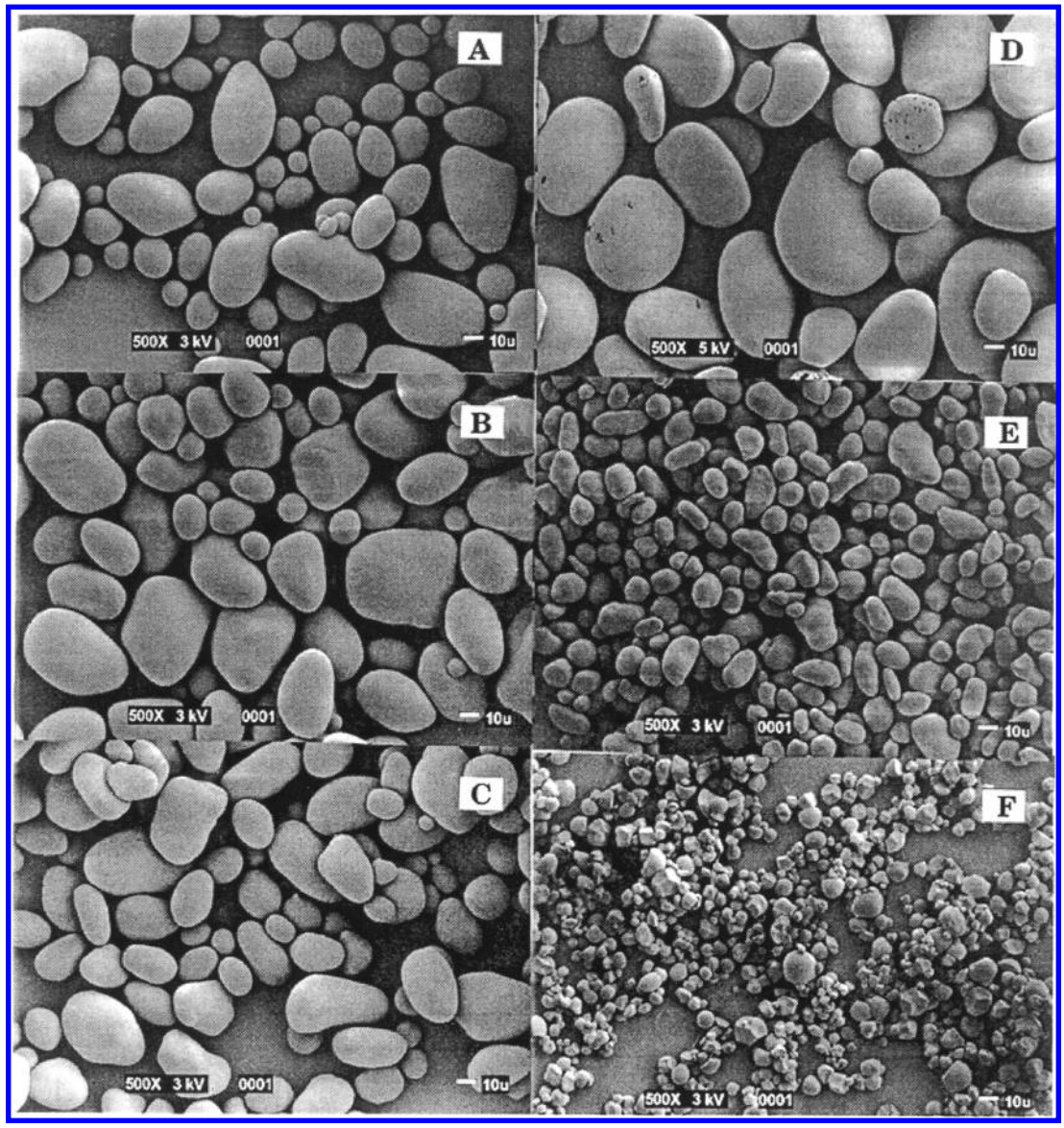

Figure 1. Scanning electron micrographs of the tuber and root starches: (**A**) potato I; (**B**) potato II; (**C**) potato III; (**D**) canna; (**E**) fern; (**F**) kudzu (scale bar = 10 μm).

and slower retrogradation rates (*3, 17*). Ong and Blanshard (*5*) reported that the texture of cooked rice was critically controlled by the proportions of the longest (DP 92−98) and short (DP ≥25) AP branch chains.

Numerous studies have been conducted to analyze the structures and properties of cereal starches. Knowledge of the structures and properties of root and tuber starches, however, is relatively limited. In this study selected root and tuber starches (potato, canna, fern, and kudzu) grown in Hangzhou, China, were characterized for their potential food and nonfood applications. Structural features of these starches, such as the branch chain length distribution and molecular weight of the AP, were studied and compared to gain more understanding of the effects of AP structures on the gelatinization, pasting, and retrogradation properties of tuber and root starches.

MATERIALS AND METHODS

Starches and Other Materials. Tuber (three different native potato varieties, I, II, and III) and root (canna, fern, and kudzu) starches were grown in Hangzhou, China. Isoamylase (EC 3.2.1.68) from *Pseudomonas amyloderamosa* was purchased from Hayashibara Biochemical Laboratories Inc. (Okayama, Japan).

Morphology of Starch. The morphology of starch was determined using scanning electron microscopy. Starch granules were mounted on brass disks with double-sided sticky tape, coated with gold/palladium (60/40), and observed using a scanning electron microscope (JEOL model 1850, Tokyo, Japan).

Crystalline Structure of Starch. Starch samples were equilibrated in a relative humidity chamber (RH 100%) at 25 °C for 24 h. X-ray diffraction patterns were obtained using nickel-filtered, Cu Kα radiation with a Siemens D-500 diffractometer (Madison, WI). Starches were scanned from 4° to 37° with a 0.05° step size and count time of 2 s.

Iodine Affinity and Amylose Content. Iodine affinities (IAs) of defatted whole starches and isolated amylopectins were determined using a potentiometric autotitrator with Meterodata recording software (702 SM Titrino, Brinkman Instrument, Westbury, NY). Apparent and absolute amylose contents were determined using the methods of Schoch (*18*) and Kasemsuwan et al. (*8*), respectively. Fractionation of starch into AM and AP was carried out following the procedures of Schoch (*19*) and Jane and Chen (*4*). Apparent AM content was calculated as $C_{app} = 100 \times IA_S/20\%$, and absolute AM content was calculated using the following equation.

$$C_{abs} = 100 \times (IA_S - IA_{AP+IC})/(20\% - IA_{AP+IC}) \quad (1)$$

C_{app}, C_{abs}, IA_S, and IA_{AP+IC} represent the percentage of apparent AM content, absolute AM content, iodine affinity of starch, and iodine

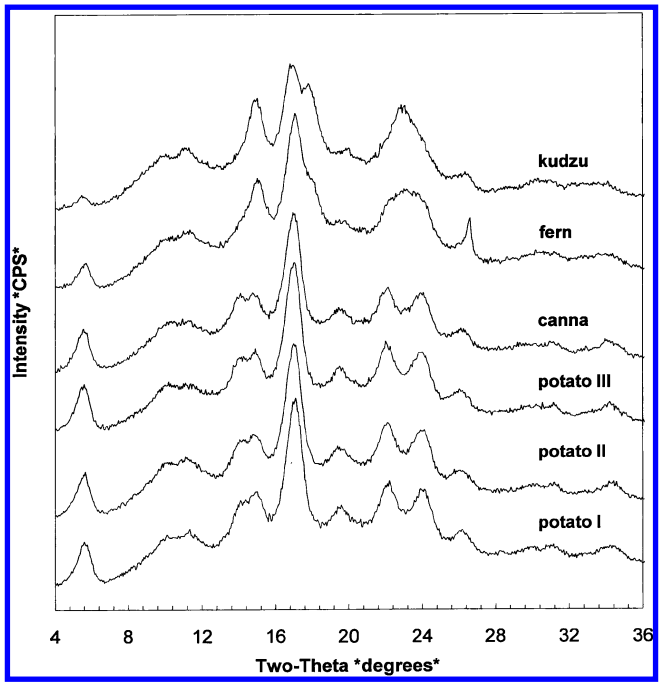

Figure 2. X-ray diffraction patterns of the tuber and root starches.

Table 1. Iodine Affinities and Amylose Contents of the Tuber and Root Starches

	iodine affinity[a] (%)		amylose content[b] (%)	
source	starch	amylopectin	apparent[c]	absolute[d]
potato I	7.5 ± 0.4	4.4 ± 0.3	37.5 ± 0.6	19.9 ± 0.5
potato II	7.0 ± 0.3	4.5 ± 0.2	35.0 ± 0.5	16.1 ± 0.4
potato III	6.4 ± 0.3	3.9 ± 0.4	32.1 ± 0.2	15.5 ± 0.3
canna	5.5 ± 0.1	1.8 ± 0.6	25.4 ± 0.6	20.3 ± 0.7
fern	5.0 ± 0.1	0.7 ± 0.2	24.9 ± 0.4	22.3 ± 0.5
kudzu	3.9 ± 0.1	0.3 ± 0.1	19.6 ± 0.2	18.3 ± 0.6

[a] Calculated, using the equation % iodine affinity = [mg of bound iodine at zero intercept/mg of sample weight (dsb)] × 100, from triplicate measurements; ± standard deviations. [b] Iodine affinity of pure amylose was 20% to calculate amylose content in starches. [c] Determined as $C_{app} = (IA_S/20\%) \times 100$ where C_{app} is the percentage of apparent amylose content and IA_S = iodine affinity of whole defatted starch. [d] Determined as $C_{abs} = 100 \times (IA_S - IA_{AP+IC})/(20\% - IA_{AP+IC})$, where C_{abs} is the percentage of absolute amylose content and IA_{AP+IC} is the iodine affinity of amylopectin and intermediate component.

Table 2. Molecular Characteristics of the Tuber and Root Amylopectins

source	X-ray pattern	M_W[a] ($\times 10^8$)	R_z[b] (nm)	ρ[c] (g/mol/nm^3)
potato I	B	1.66 ± 0.17	379.7 ± 76.0	3.02
potato II	B	1.18 ± 0.38	358.3 ± 76.2	2.56
potato III	B	0.87 ± 0.19	242.5 ± 30.7	6.07
canna	B	0.20 ± 0.10	247.2 ± 12.8	1.38
fern	C	2.63 ± 0.00	283.3 ± 29.3	11.55
kudzu	C_A	2.05 ± 0.02	247.6 ± 13.2	13.48

[a] Weight-average molecular weight. [b] z-average radius of gyration. [c] Dispersed molecular density (ρ) = M_W/R_z^3.

affinity of a mixture of AP and intermediate component (IC), respectively. The intermediate component is starch molecules that have branched structures resembling AP but smaller molecular weight, similar to AM. The IA of isolated amylose was 20%.

Molecular Weight Distribution of Starch by Gel Permeation Chromatography (GPC). Sample preparation and GPC analysis were carried out following the method described previously (*20*). Separation using a Sepharose CL-2B gel (Pharmacia Inc., Piscataway, NJ) column was achieved with an eluent containing 10 mM NaOH and 50 mM NaCl with a flow rate of 30 mL/h. Fractions were collected, and the total carbohydrate (CHO) contents and blue values (BV) were determined using an ultra microplate reader (Bio-Tek Instruments Inc., Winooski, VT) following the procedures of Dubois et al. (*21*), Fox and Robyt (*22*), and Jane and Chen (*4*), with some modifications.

Absolute Molecular Weight of AP by HPSEC-MALLS-RI System. Instrumental details and the method of data analysis for determining the molecular weight of AP were reported previously in Yoo and Jane (*1*). Briefly, high-performance size exclusion chromatographic (HPSEC) analysis combined with multiangle laser-light scattering (MALLS; Dawn DSP-F, Wyatt Technology Corp., Santa Barbara, CA) and refractive index (RI; HP 1047A, Hewlett-Packard, Valley Forge, PA) detectors was applied for this purpose. Shodex OH pak KB-G guard and KB-806 and KB-804 analytical columns (Showa Denko K.K., Tokyo, Japan) were used to obtain the AP molecular weight distribution. The mobile phase was distilled−deionized water (18.2 MΩ cm), and the flow rate was 0.7 mL/min.

Data obtained from MALLS and RI detectors were analyzed using Astra software (version 4.7.07, Wyatt Technology Corp.). The second-order Berry method was used in this study for curve fitting of laser-light scattering signals from multiangle detectors.

Branch Chain Length Distribution of AP. Isolated APs were debranched using isoamylase according to the procedure of Jane and Chen (*4*), and branch chain length distributions were obtained by using a high-performance anion exchange chromatograph with a postcolumn amyloglucosidase reactor and a pulsed amperometric detector (HPAEC-ENZ-PAD) (*23*). The separation of samples was carried out using a PA-100 anion exchange analytical column and a PA-100 guard column (Dionex, Sunnyvale, CA). The mobile phase used for separation consisted of eluent A (100 mM NaOH) and eluent B (100 mM NaOH and 300 mM $NaNO_3$) with a flow rate of 0.5 mL/min. The separation gradient was programmed as follows: 0−5 min, 99% A and 1% B; 5−30 min, linear gradient to 8% B; 30−150 min, linear gradient to 30% B; 150−200 min, linear gradient to 45% B.

Naegeli Dextrins Prepared by Acid Hydrolysis of Starch. Naegeli dextrins of starches were prepared by hydrolyzing granular starch with a H_2SO_4 solution (15.3%, v/v) at 40 °C for 12 days, following the procedure of Jane et al. (*24*). HPAEC-ENZ-PAD chromatograms of Naegeli dextrins (12-day hydrolysis) were obtained following the procedure stated earlier.

Thermal Properties of Starch. Thermal properties of starches were determined using a differential scanning calorimeter equipped with an Intracooler II system and Pyris thermal analysis software (DSC-7, Perkin-Elmer Corp., Norwalk, CT). Starch (2 mg) and water (6 μL) were sealed in an aluminum pan and equilibrated at room temperature for 2 h. The sample was scanned from 25 to 100 °C at a heating rate of 10 °C/min using an empty pan as the reference. The analysis of retrograded starch was carried out following the same method after gelatinized samples had been stored at 4 °C for 7 days.

Phosphorus Contents of Starch. Phosphorus contents of starches were determined by using a colorimetric chemical method (*25*).

Pasting Properties. Pasting profiles of starches were obtained using an RVA-4 Rapid Visco-Analyzer (Newport Scientific Pty. Ltd., Warriewood, NSW, Australia). Starch suspensions (8%, dsb) were equilibrated at 50 °C for 1 min at a stirring rate of 160 rpm, heated to 95 °C at a rate of 6 °C/min, held at 95 °C for 5 min, and cooled to 50 °C at a rate of 6 °C/min. The sample was stirred at 160 rpm throughout the analysis.

RESULTS AND DISCUSSION

Scanning electron micrographs of root and tuber starches displayed unique granular shapes and sizes depending on botanical sources (**Figure 1**). Starches from all three potato varieties showed oval and spherical granules with smooth surfaces, and the granule size was in the range of 10−100 μm. Potato I (**Figure 1A**) had a larger population of small granules than the other two potato starches (**Figure 1B**,**C**). Canna starch (**Figure 1D**) had ellipsoidal, oval, and spherical granules with diameters of 30−110 μm, which made canna starch the largest known starch granules (*26*). The morphology of potato and

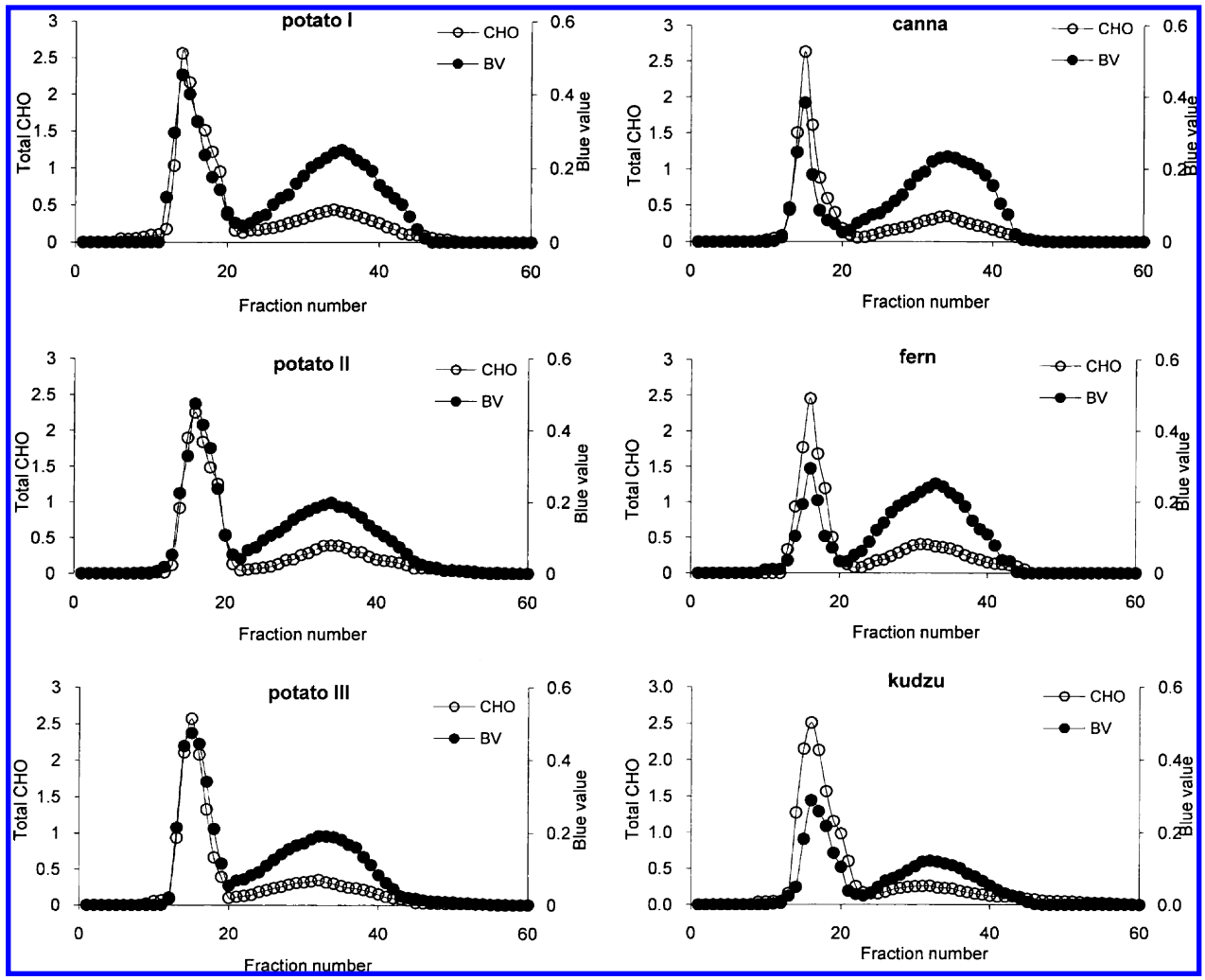

Figure 3. Gel permeation chromatograms of the tuber and root starches using a Sepharose CL-2B column. CHO, total carbohydrate content determined by phenol−sulfuric acid method; BV, blue value determined by iodine absorption at 640 nm.

Table 3. Branch Chain Length Distributions of the Tuber and Root Amylopectins

source	peak DP		av chain length (DP)	% distribution of DPs				highest detectable DP
	I	II		6−12	13−24	25−36	≥37	
potato I	14	49	30.7 ± 0.8	12.8 ± 0.8	38.6 ± 0.4	13.6 ± 0.8	34.8 ± 0.8	85
potato II	14	49	31.3 ± 0.7	10.6 ± 0.5	39.5 ± 0.6	15.1 ± 0.9	34.6 ± 0.5	85
potato III	14	49	30.5 ± 0.8	11.2 ± 0.7	40.1 ± 0.7	15.4 ± 0.9	33.3 ± 0.6	82
canna	14	48	28.5 ± 0.5	13.1 ± 0.8	43.9 ± 0.5	13.7 ± 0.6	29.3 ± 0.2	83
fern	13	46	27.4 ± 0.8	16.5 ± 0.2	41.8 ± 0.9	13.0 ± 0.3	28.6 ± 0.4	75
kudzu	12	46	25.1 ± 0.7	18.3 ± 0.8	46.2 ± 0.2	12.9 ± 0.7	22.5 ± 0.7	75

canna starch granules was in agreement with that reported in the literature (*26*). A few granules of canna starch displayed tiny pinholes (**Figure 1D**), which were attributed to a result of enzyme hydrolysis. Fern starch (**Figure 1E**) displayed rod- and irregular-shaped granules with smaller sizes (3−30 μm). Kudzu starch (**Figure 1F**) had much smaller granules (3−15 μm) with polygonal and spherical shapes. The shape and the size of the kudzu starch resembled those of winter squash starch (*27*).

X-ray diffraction patterns of the starches are shown in **Figure 2**. Potato I, II, and III and canna starches showed typical B-type X-ray patterns with strong peak intensities. Fern starch showed a C-type pattern, whereas kudzu starch showed a C_A pattern, which was closer to the A-pattern than the B-pattern.

Iodine affinities and amylose (AM) contents of defatted starches are given in **Table 1**. Among potato starches, potato I showed the largest apparent (37.5%) and absolute (19.9%) AM contents, and potato III showed the least: 32.1 and 15.5%, respectively. It is known that B-type starches have APs with more long branch chains. These chains also form helical complexes with iodine and give overestimated AM contents. The substantially larger apparent AM contents by iodine affinity of the potato starches were attributed to their large proportions of long branch chains. For example, the absolute AM content of the fern starch was larger than that of all of the potato starches, even though the iodine affinity of the fern starch (5.0%) was smaller than those of potato starches (6.4−7.5%). The fern starch, with a C-type polymorph, had the largest absolute AM content (22.3%) because of its short AP branch chains and low iodine affinity of AP (0.7%). Kudzu, with a C_A-type polymorph, had the smallest iodine affinity of AP (0.3%), resulting from its very short branch chains and the lowest apparent AM content (19.6%).

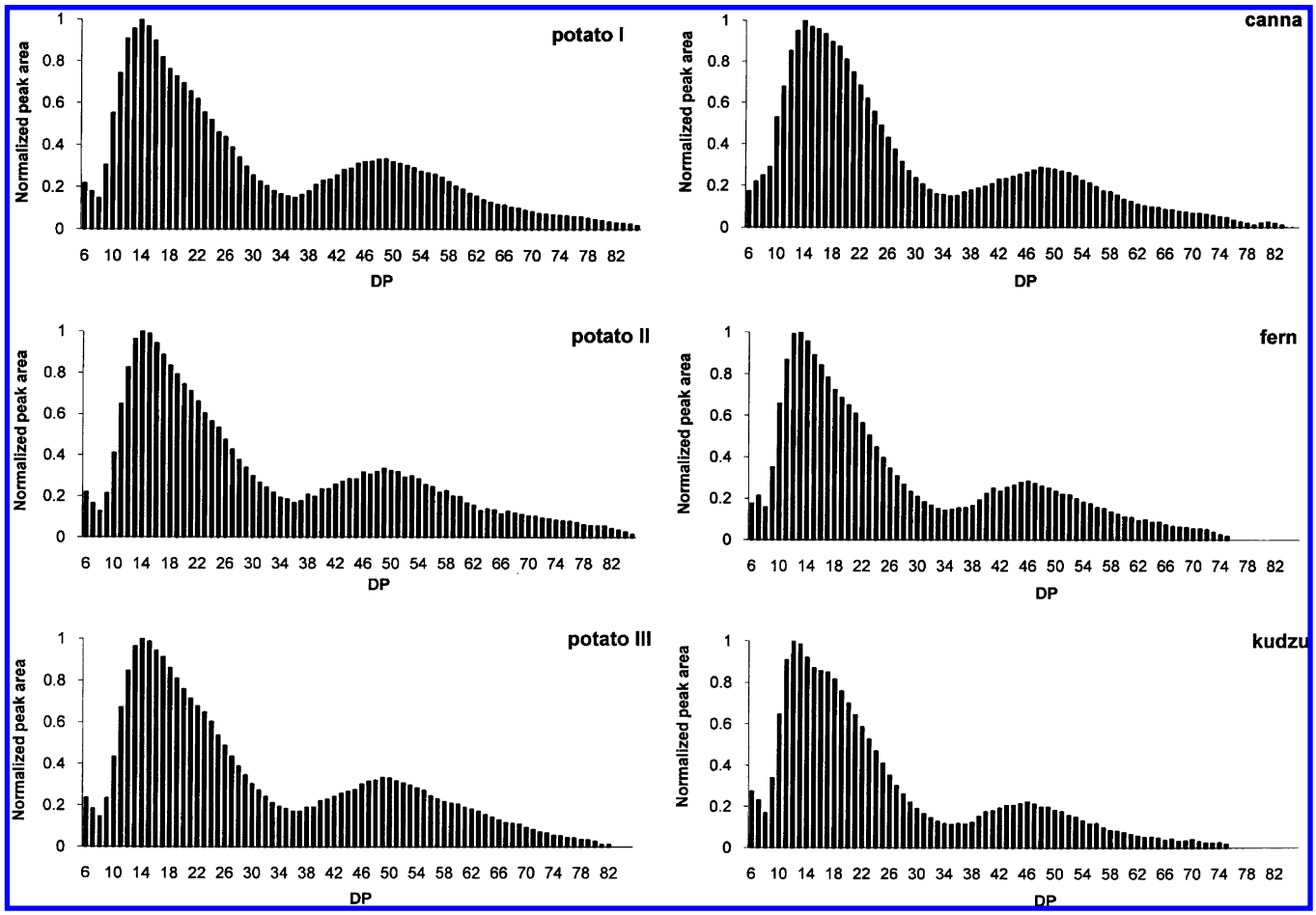

Figure 4. Chain length distributions of isoamylase-debranched tuber and root amylopectins.

Molecular weight distributions of the starches obtained by GPC displayed two distinct peaks representing AP (the first peak) and AM (the second peak) (**Figure 3**). These results reflected a discrepancy between the apparent and absolute AM contents of starches. All three potato starches showed substantially larger blue values for their AP peaks than other starches, which indicated the formation of an iodine complex with longer AP branch chains. These results were consistent with the large iodine affinity for potato AP shown in **Table 1**. Kudzu and fern starches showed smaller blue values of AP peaks, indicating shorter AP branch chains.

Weight-average molecular weights (M_w) and *z*-average radii of gyration (R_z) of the APs of root and tuber starches are shown in **Table 2**. The results showed that M_w values of potato APs were (0.87−1.66) × 10^8 g/mol. Fern AP of a C-type starch displayed the largest M_w (2.63 × 10^8 g/mol) of all the starches, whereas canna AP (B-type) had the smallest M_w (2.04 × 10^7 g/mol). The R_z values of APs were in the range of 242.5−379.7 nm. The dispersed molecular densities of the C- and C_A-type APs (11.6−13.5 g/mol/nm^3) were larger than those of the B-type APs (1.4−6.1 g/mol/nm^3). These results were consistent with previous results in that dispersed molecular densities of B-type APs (2.9−5.3 g/mol/nm^3) were smaller than those of the A-type APs (7.2−16.1 g/mol/nm^3) (*1*). The C-type polymorph of starch has been proposed to be a mixture of the A- and B-types (*28, 29*). Bogracheva et al. reported that pea starch granules of a C-type polymorph consisted of B-type polymorphs in the center of the granule surrounded by the A-type polymorphs (*30*). The results obtained from this study showed that the AP of the C-type polymorphic starch had a mixed branch structure of the A- and B-type polymorphic starches.

Branch chain length distribution resulting from the debranching of APs is shown in **Figure 4** and summarized in **Table 3**. All potato APs showed their first chain length peak at DP 14 and the second peak at DP 49. Canna, fern, and kudzu had the first peak at DP 14, 13, and 12 and the second peak at DP 48, 46, and 46, respectively. A valley at DP 8 that is characteristic of potato APs, and some other root starches (*14, 31*), was observed in all chromatograms except for canna. Fern AP had a larger proportion of DP 7 than of DP 6, but the valley was at DP 8. B-type starches are known to have lower percentages of short chains (DP 6−12) and more long chains (DP ≥37) (*3, 9, 14*). Potato I, II, and III and canna, which showed the B-type X-ray patterns, had 10.6−12.8% short chains (DP 6−12) and 29.3−34.8% long chains (DP ≥37) (**Table 3**). Fern and kudzu APs had more short chains (DP 6−12) (15.6 and 18.3%, respectively) than did the B-type starches, but fewer than did most A-type starches (*3*). Potato APs had average chain lengths in the range of DP 30.5−31.3, and that of canna was DP 28.5. The longest detectable chains of the B-type starches (potato I, II, and III and canna) were in the range of DP 82−85, whereas both kudzu (C_A-pattern) and fern (C-pattern) had DP 75. Of these starches, kudzu AP had the smallest average chain length (DP 25.1), the largest proportion (18.3%) of short chains (DP 6−12), and the smallest proportion (22.5%) of long chains (DP ≥37) of the other APs. Takeda et al. (*32*) reported that APs with higher iodine affinities had a larger proportion of long branch chains and a smaller proportion of short chains than APs with low iodine affinities. The higher iodine affinities of the potato APs and the lower iodine affinities of fern and kudzu APs are clearly explained by their branch chain length distributions.

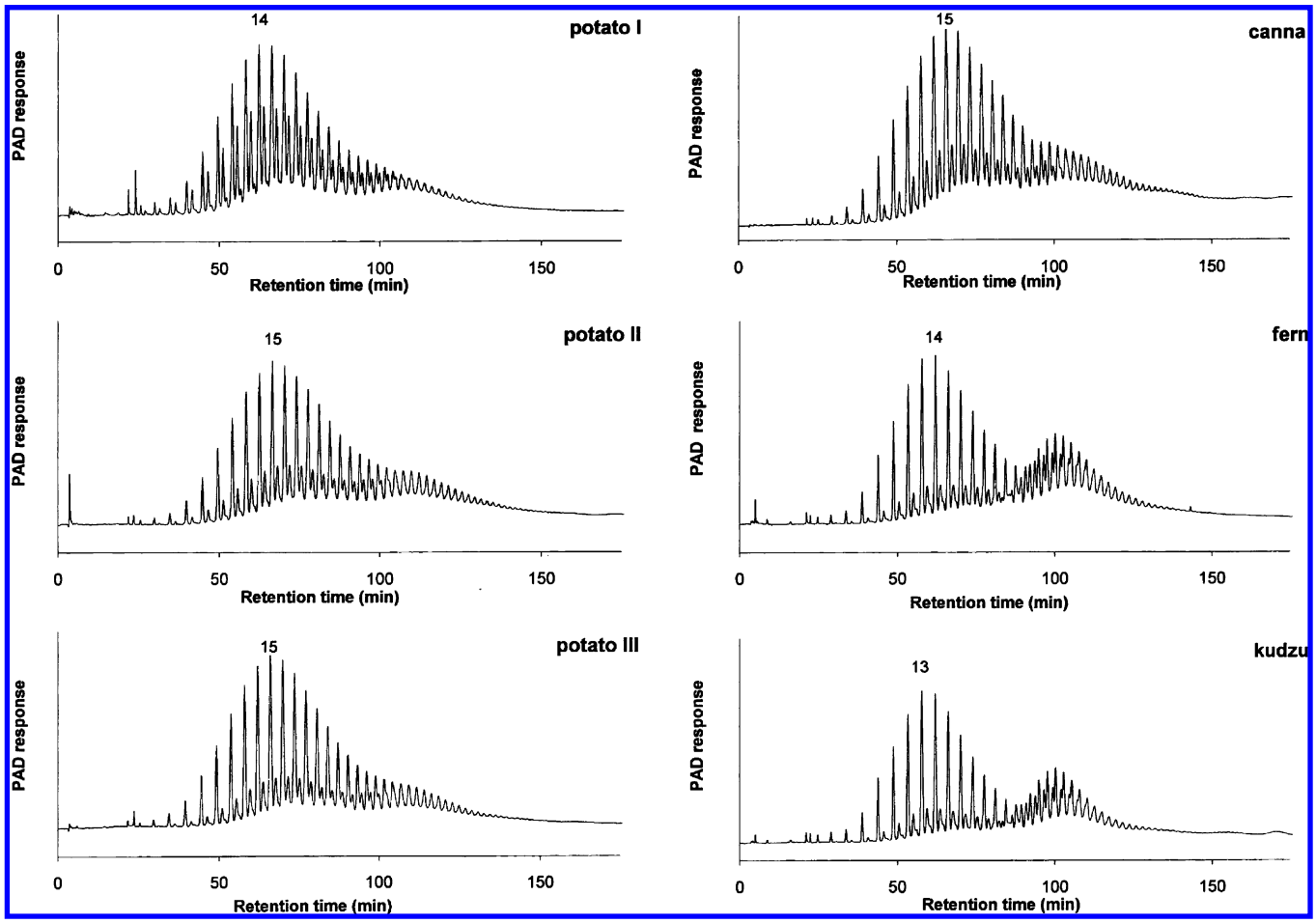

Figure 5. High-performance anion exchange chromatograms of Naegeli dextrins obtained after 12 days of acid hydrolysis.

Table 4. Gelatinization Properties of the Tuber and Root Starches

source	gelatinization temperatures[a] (°C) T_o	T_p	T_c	ΔH[b] (J/g)
potato I	62.1 ± 0.1	65.8 ± 0.3	70.4 ± 0.4	19.5 ± 0.4
potato II	62.3 ± 0.4	65.8 ± 0.1	71.7 ± 0.2	19.5 ± 0.1
potato III	62.9 ± 0.2	67.7 ± 0.7	73.3 ± 0.3	19.0 ± 0.5
canna	62.7 ± 0.1	67.7 ± 0.1	72.9 ± 0.2	19.1 ± 0.1
fern	60.7 ± 0.2	65.8 ± 0.4	72.4 ± 0.5	16.3 ± 0.4
kudzu	63.3 ± 0.6	71.3 ± 0.1	76.8 ± 0.4	14.4 ± 0.3

[a] T_o, T_p, and T_c represent onset, peak, and conclusion temperatures of gelatinization endotherms. [b] ΔH stands for enthalpy change during starch gelatinization. Values are averages of triplicate measurements.

Table 5. Properties of the Retrograded Tuber and Root Starches[a]

source	T_o (°C)	T_p (°C)	T_c (°C)	ΔH[b] (J/g)	% R[c]
potato I	40.5 ± 0.6	55.1 ± 0.8	66.3 ± 0.4	8.1 ± 0.5	41.5
potato II	42.0 ± 1.4	56.7 ± 0.4	68.9 ± 0.3	7.9 ± 0.0	40.5
potato III	40.8 ± 0.9	57.2 ± 0.9	68.3 ± 0.5	6.8 ± 0.1	35.8
canna	42.5 ± 0.4	54.0 ± 0.4	65.6 ± 0.2	5.2 ± 0.1	27.2
fern	39.7 ± 0.9	51.8 ± 0.7	60.8 ± 0.4	4.7 ± 0.5	28.8
kudzu	37.9 ± 0.4	51.0 ± 0.9	60.7 ± 0.1	6.4 ± 0.3	44.4

[a] T_o, T_p, and T_c represent onset, peak, and conclusion temperatures of gelatinization endotherm. [b] ΔH is enthalpy change of starch retrogradation at 4 °C for 7 days. [c] Degree of retrogradation (% R) = ΔH(gelatinization of retrograded starch)/ΔH(gelatinization of native starch) × 100.

Naegeli dextrins of starches were prepared by acid hydrolysis at 40 °C for 12 days. The chain-length profiles of the Naegeli dextrins displayed the first major peaks of linear chains followed by the second peaks of singly branched chains (**Figure 5**). Potato I, II, and III, canna, fern, and kudzu had their first chain-length peaks at DP 14, 15, 15, 15, 14, and 13, respectively. Naegeli dextrins of the C- and C_A-type starches had more prominent second peaks than the B-type starches, indicating that there was a substantial amount of singly branched molecules remaining in the former. It has been proposed that short branch chains of the C- and A-type starch APs have branch linkages located within the double-helical crystalline lamella and are protected from acid hydrolysis (*24*), whereas the B-type starch APs have fewer branch linkages, and most of the linkages are located in the amorphous region and are easily hydrolyzed by acid (*24*). After an isoamylase debranching reaction, the second peak, consisting of singly branched molecules, disappeared, with the linear chain peak becoming larger (**Figure 6**).

Thermal properties of the root and tuber starches were analyzed using differential scanning calorimetry (DSC). The onset gelatinization temperatures (T_o) of all the starches were in a range of 60.7−63.3 °C (**Table 4**). Potato and canna starches showed larger gelatinization enthalpy changes (ΔH) of 19.0−19.5 J/g because of their long branch chains involved in the crystallite. Larger proportions of long branch chains in potato APs led to an increase in the size of crystalline lamella, which contributed to the larger ΔH values of potato starches. Canna starch displayed T_o and ΔH values very similar to those of potato starches and also contained a fairly large proportion of long branch chains. Kudzu starch showed a slightly higher T_o of 63.3 °C and the lowest ΔH of 14.4 J/g among the starches analyzed. It is plausible that the larger proportion (18.3%) of short chains of DP 6−12 and comparatively smaller proportion (22.5%) of long branch chains in kudzu AP resulted in a lower gelatinization

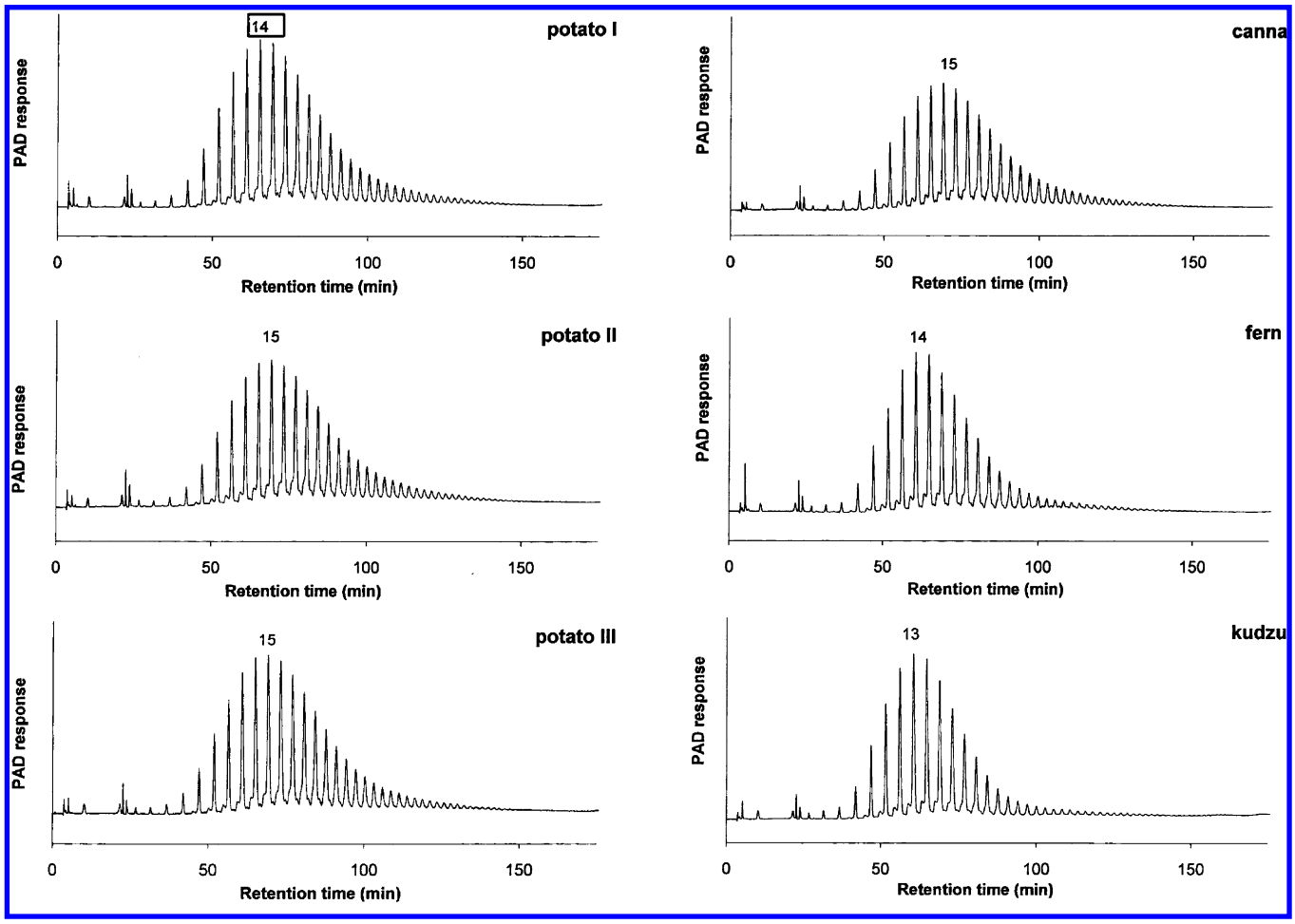

Figure 6. High-performance anion exchange chromatograms of isoamylase-debranched Naegeli dextrins.

Table 6. Phosphorus Contents and Pasting Properties of the Tuber and Root Starches

starch	phosphorus content (%)	peak (RVU)	breakdown viscosity (RVU)	final viscosity (RVU)	set back (RVU)	pasting temperature (°C)
potato I	0.042 ± 0.002	589.6 ± 16.7	405.4 ± 17.3	260.1 ± 0.5	76.0 ± 1.0	65.3 ± 0.2
potato II	0.083 ± 0.002	749.0 ± 24.9	511.4 ± 14.2	318.1 ± 6.5	80.1 ± 4.6	66.8 ± 0.4
potato III	0.059 ± 0.001	550.3 ± 14.8	320.3 ± 9.5	316.9 ± 7.1	86.9 ± 1.8	68.7 ± 0.0
canna	0.046 ± 0.001	115.7 ± 1.9	42.2 ± 0.3	107.6 ± 3.1	34.2 ± 1.6	69.6 ± 0.1
fern	0.008 ± 0.001	328.8 ± 1.5	175.1 ± 4.4	258.8 ± 2.8	105.2 ± 0.3	66.9 ± 0.2
kudzu	0.014 ± 0.002	211.6 ± 6.6	99.8 ± 3.3	210.3 ± 6.5	98.4 ± 3.1	73.2 ± 0.0

ΔH. It is likely that more branching points located in the crystalline lamella could result in inferior crystalline structures of A- and C-type starches as discussed in Jane et al. (*24*). Thus, this could be another reason that C- and C_A-type starches, which had mixed crystalline structures of A- and B-polymorphs, had relatively smaller ΔH values than did B-type starches.

Starch retrogradation is defined to be recrystallization of dispersed starch molecules. Properties of retrograded root and tuber starches are given in **Table 5**. All retrograded starches showed considerably lower onset temperatures (37.9−42.5 °C) than the onset gelatinization temperatures (60.7−63.3 °C) of their native starches. The degree of retrogradation of starches was in the range from 27.2% (canna) to 44.4% (kudzu). Potato starches analyzed in this study had similar degrees of retrogradation as those in previous studies (*3, 17*). The percentage retrogradation of potato starches decreased in the order potato I > potato II > potato III, which followed the same order as the amylose contents of the starches. It is known that amylose is prompt to crystallize (*3*). Canna starch had the lowest degree of retrogradation (27.2%) and kudzu starch had the highest (44.4%) among the starches. Canna starch was expected to have a similar degree of retrogradation as other B-type starches, but the enzymatic damage to the starch granule might affect its physical properties. The SEM image of canna starch suggested that a few granules were attacked by amylase-type enzymes as mentioned earlier (**Figure 1**). The large phosphate-monoester contents of the B-type starches (**Table 6**) also reduced their retrogradation rates.

Pasting properties are influenced by the AM content, branch chain-length distribution of AP, phosphate-monoester derivatives, and lipids. APs contribute to the swelling of starch granules, and AM and lipids inhibit swelling (*33*). Jane and Chen (*4*) reported that AM molecular size and AP branch chain-length distribution produced synergistic effects on viscosity of starch pastes. In general, tuber and root starches showed low pasting temperatures, lower resistance to shear thinning, and lower setback viscosities than cereal starches (*3*), which were mainly attributed to the absence of lipids and the presence of phosphate-monoester derivatives. Pasting properties of the starches are given in **Figure 7** and **Table 6**. Potato starches had lower pasting temperatures (65.3−68.7 °C) and significantly higher peak viscosities (550.3−749.0 RVU), resulting from substantial

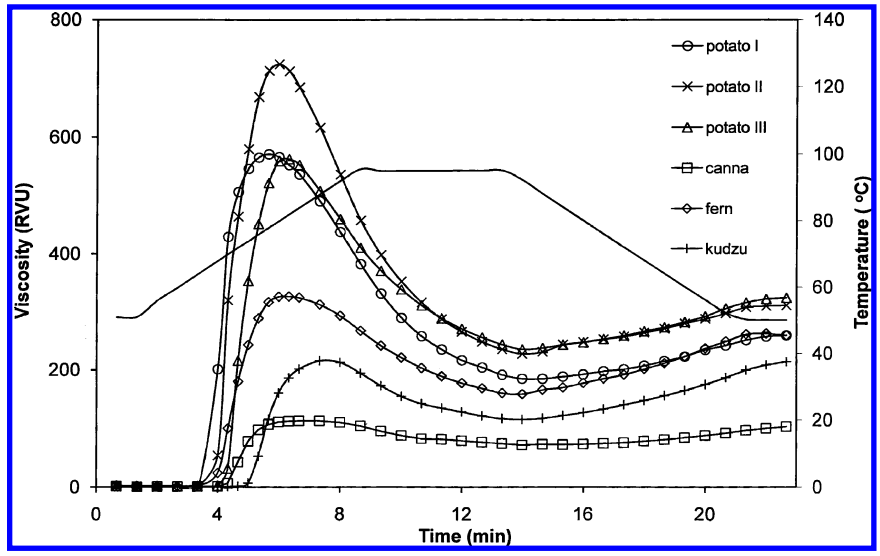

Figure 7. Rapid Visco-Analyzer pasting profiles of the tuber and root starches (8% dsb).

amounts of phosphate monoesters, long AP branch chains, and large granule sizes, which were different from cereal and other B-type starches (*3*). Potato II starch, which had the largest phosphate-monoester content, displayed the highest peak viscosity (**Table 6**). Other root starches, such as fern and kudzu, contained much smaller amounts of phosphate monoesters and showed lower peak viscosities as expected (**Table 6**). Unexpectedly, canna starch had a very low peak viscosity, which contradicted the previously reported results of high peak viscosity (183−258 RVU) and set-back viscosities even at 5−6% suspension (*3, 34*). The above-mentioned pinholes in the granules (**Figure 1D**) and very small AP M_W (**Table 2**) caused by endogenous enzymatic hydrolysis could have resulted in such a low viscosity (116 RVU). Kudzu starch displayed the highest pasting temperature (73.2 °C) among the starches. It is plausible that the small starch granules had limited swelling capacity, which retarded the development of viscosity and resulted in pasting at higher temperature. Fern starch with substantially larger absolute AM content had the highest set-back viscosity, which was a result of AM molecules leaching from swollen granules during heating reassociating to form a network during the cooling process and gave a large set-back viscosity.

The results obtained from this study suggested that potato II starch provided the highest viscosity, which would be a good choice as a thickening agent. Kudzu starch, which gave a low viscosity, would be useful for applications requiring high starch concentrations and low viscosity. Fern starch displayed a low retrogradation rate, which would have advantages for making dessert-like products that maintained a soft texture with a slow staling process, yielding an extended shelf life. The results also extended our knowledge on how the structures, including AM content, branch chain length of AP, and phosphate monoesters, affected gelatinization, pasting, and retrogradation properties of tuber and root starches.

ABBREVIATIONS USED

DP, degree of polymerization; SEM, scanning electron microscopy; GPC, gel permeation chromatography; HPSEC, high-performance size exclusion chromatography; MALLS, multiangle laser-light scattering; HPAEC, high-performance anion exchange chromatography; PAD, pulsed amperometric detector; M_w, weight-average molecular weight; R_z, *z*-average radius of gyration; AM, amylose; AP, amylopectin; CHO, carbohydrate; BV, blue value; dsb, dry starch basis; RVU, Rapid Visco-analyzer unit; RI, refractive index.

ACKNOWLEDGMENT

We thank Dr. Arland Hotchkiss for reviewing thr manuscript, Bessey Microscopy Facilities at Iowa State University for the SEM study, and Dr. Scott Schlorboltz for the X-ray analysis.

LITERATURE CITED

(1) Yoo, S.-H.; Jane, J. Molecular weights and gyration radii of amylopectins determined by high-performance size-exclusion chromatography equipped with multi-angle laser-light scattering and refractive index detectors. *Carbohydr. Polym.* **2002**, *49*, 307–314.

(2) Hizukuri, S. Polymodal distribution of the chain lengths of amylopectins, and its significance. *Carbohydr. Res.* **1986**, *147*, 342–347.

(3) Jane, J.; Chen, Y. Y.; Lee, L. F.; McPherson, A. E.; Wong, K. S.; Radosavljevic, M. Effects of amylopectin branch chain length and amylose content on the gelatinization and pasting properties of starch. *Cereal Chem.* **1999**, *76*, 629–637.

(4) Jane, J.; Chen, J.-F. Effect of amylose molecular size and amylopectin branch chain length on paste properties of starch. *Cereal Chem.* **1992**, *69*, 60–65.

(5) Ong, M. H.; Blanshard, M. V. Texture determinants in cooked, parboiled rice. I. Rice starch amylose and the fine structure of amylopectin. *J. Cereal Sci.* **1995**, *21*, 251–260.

(6) Takeda, Y.; Maruta, N.; Hizukuri, S.; Juliano, B. O. Structure of indica rice starch (IR 48 and IR 64) having intermediate affinities for iodine. *Carbohydr. Res.* **1992**, *187*, 287–294.

(7) Blanshard, J. M. V. Starch granule structure and function: a physicochemical approach In *Starch Properties and Potential*; Galliard, T., Ed.; Wiley: New York, 1987; pp16−19.

(8) Kasemsuwan, T.; Jane, J.; Schnable, P.; Stinard, P.; Robertson, D. Characterization of the dominant amylose-extender (Ael-5180) maize starch. *Cereal Chem.* **1995**, *72*, 457–464.

(9) Hizukuri, S.; Kaneko, T.; Takeda, Y. Measurements of the chain length of amylopectin and its relevance to the origin of crystalline polymorphism of starch granules. *Biochim. Biophys. Acta* **1983**, *760*, 188–191.

(10) Hizukuri, S.; Takeda, Y.; Usami, S.; Takase, Y. Effect of aliphatic hydrocarbon groups on the crystallization of amylodextrin: model experiments for starch crystallization. *Carbohydr. Res.* **1980**, *83*, 193–199.

(11) Whittam, M. A.; Noel, T. R.; Ring, S. G. Melting behavior of A- and B-type crystalline starch. *Int. J. Biol. Macromol.* **1990**, *12*, 359–362.

(12) Gallant, D. J.; Bouchet, B.; Buleon, A.; Perez, S. Physical characteristics of starch granules and susceptibility to enzymatic degradation. *Eur. J. Clin. Nutr.* **1992**, *46*, S3–S16.
(13) Hizukuri, S. Relationship between the distribution of the chain length of amylopectin and the crystalline structure of starch granules. *Carbohydr. Res.* **1985**, *141*, 295–310.
(14) Hanashiro, I.; Abe, J.; Hizukuri, S. A periodic distribution of the chain length of amylopectin as revealed by high-performance anion exchange chromatography. *Carbohydr. Res.* **1996**, *283*, 151–159.
(15) Asaoka, M.; Okuno, K.; Fuwa, H. Effect of environmental temperature at the milky stage on amylose content and fine structure of amylopectin of waxy and nonwaxy endosperm starches of rice. *Agric. Biol. Chem.* **1985**, *49*, 373–379.
(16) Yuan, R. C.; Tompson, D. B.; Boyer, C. D. Fine structure of amylopectin in relation to gelatinization and retrogradation behavior of maize starches from three *wx*-containing genotypes in two inbred lines. *Cereal Chem.* **1993**, *70*, 81–89.
(17) McPherson, A. E.; Jane, J. Comparison of waxy potato with other root and tuber starches. *Carbohydr. Polym.* **1999**, *40*, 57–70.
(18) Schoch, T. J. Iodimetric determination of amylose. Potentiometric titration: Standard method In *Methods in Carbohydrate Chemistry: Starch*; Whistler, R. L., Smith, R. J., BeMiller, J. N., Wolformm M. L., Eds.; Academic Press: London, U.K., 1964; Vol. IV, pp157−160.
(19) Schoch, T. J. Fractionation of starch by selective precipitation with butanol. *J. Am. Chem. Soc.* **1942**, *64*, 2954–2956.
(20) Yoo, S.-H.; Jane, J. Structural and physical characteristics of waxy and other wheat starches. *Carbohydr. Polym.* **2002**, *49*, 297–305.
(21) Dubois, M.; Gilles, K. A.; Hamilton, J. K.; Rebers, P. A.; Smith, F. Colorimetric method for determination of sugars and related substances. *Anal. Chem.* **1956**, *28*, 350–356.
(22) Fox, J. D.; Robyt, J. F. Miniaturization of three carbohydrate analyses using Microsample plate reader. *Anal. Chem.* **1991**, *195*, 93–96.
(23) Wong, K.-S.; Jane, J. Quantitative analysis of debranched amylopectin by HPAEC-PAD with a postcolumn enzyme reactor. *J. Liq. Chromatogr. Relat. Technol.* **1997**, *20*, 297–310.
(24) Jane, J.; Wong, K.-S.; McPherson, A. E. Branch-structure difference in starches of A- and B-type X-ray patterns revealed by their Naegeli dextrins. *Carbohydr. Res.* **1997**, *300*, 219–227.
(25) Smith, R. J.; Caruso, J. Determination of phosphorous. In *Methods in Carbohydrate Chemistry*; Whistler, R. L., Ed.; Academic Press: Orlando, FL, 1964; Vol. 4, pp 42−46.
(26) Jane, J.; Kasemsuwan, T.; Leas, S.; Zobel, H.; Robyt, J. F. Anthology of starch granule morphology by scanning electron microscopy. *Starch/Staerke* **1994**, *46*, 121–129.
(27) Stevenson, D. G.; Yoo, S.-H.; Hurst, P. L.; Jane, J. Structural and physichochemical characteristics of winter squash (*Cucurbita maxima* D.) fruits starches at harvest. *Carbohydr. Polym.* **2005**, *59*, 153–163.
(28) Sarko, A.; Wu, H. C. H. The crystal structures of A-, B-, and C-type polymorphs of amylose and starch. *Starch/Staerke* **1978**, *30*, 73–78.
(29) Zobel, H. F. Starch crystal transformations and their industrial importance. *Starch/Staerke* **1988**, *40*, 1–7.
(30) Togracheva, T. Y.; Morris, V. J.; Ring, S. G.; Hedley, C. L. The granular structure of C-type pea starch and its role in gelatinization. *Biopolymers* **1998**, *45*, 323–332.
(31) Koizumi, K.; Fukuda, M.; Hizukuri, S. Estimation of the distributions of chain length of amylopectins by high-performance liquid chromatography with pulsed amperometric detection. *J. Chromatogr.* **1991**, *585*, 233–238.
(32) Takeda, Y.; Hizukuri, S.; Juliano, B. O. Structure of rice amylopectins with low and high affinities for iodine. *Carbohydr. Res.* **1987**, *168*, 79–88.
(33) Tester, R. T.; Morrison, W. R. Swelling and gelatinization of cereal starches. I. Effect of amylopectin, amylose and lipids. *Cereal Chem.* **1990**, *67*, 551–557.
(34) Thitipraphunkul, K.; Uttapap, D.; Piyachomkwan, K.; Takeda, Y. A comparative study of edible canna (*Canna edulis*) starch from different cultivars. Part I. Chemical composition and physicochemical properties. *Carbohydr. Polym.* **2003**, *53*, 317–324.

Received for review September 22, 2008. Revised manuscript received December 11, 2008. Accepted December 15, 2008.

JF802960F